



HAL
open science

A harmonic framework for the identification of linear time-periodic systems

Flora Vernerey, Pierre Riedinger, Andrea Iannelli, Jamal Daafouz

► **To cite this version:**

Flora Vernerey, Pierre Riedinger, Andrea Iannelli, Jamal Daafouz. A harmonic framework for the identification of linear time-periodic systems. 2023. hal-04218441v1

HAL Id: hal-04218441

<https://hal.science/hal-04218441v1>

Preprint submitted on 26 Sep 2023 (v1), last revised 16 Apr 2024 (v2)

HAL is a multi-disciplinary open access archive for the deposit and dissemination of scientific research documents, whether they are published or not. The documents may come from teaching and research institutions in France or abroad, or from public or private research centers.

L'archive ouverte pluridisciplinaire **HAL**, est destinée au dépôt et à la diffusion de documents scientifiques de niveau recherche, publiés ou non, émanant des établissements d'enseignement et de recherche français ou étrangers, des laboratoires publics ou privés.

A harmonic framework for the identification of linear time-periodic systems

Flora Vernerey, Pierre Riedinger, Andrea Iannelli and Jamal Daafouz

Abstract—This paper presents a novel approach for the identification of linear time-periodic (LTP) systems in continuous time. This method is based on harmonic modeling and consists in converting any LTP system into an equivalent LTI system with infinite dimension. Leveraging specific harmonic properties, we demonstrate that solving this infinite-dimensional identification problem can be reduced to solving a finite-dimensional linear least-squares problem. The result is an approximation of the original solution with an arbitrarily small error. Our approach offers several significant advantages. The first one is closely tied to the harmonic system’s inherent LTI characteristic, along with the Toeplitz structure exhibited by its elements. The second advantage is related to the regularization property achieved through the integral action when computing the phasors from input and state trajectories. Finally, our method avoids the computation of signals’ derivative. This sets our approach apart from existing methods that rely on such computations, which can be a notable drawback, especially in continuous-time settings. We provide numerical simulations that convincingly demonstrate the effectiveness of the proposed method, even in scenarios where signals are corrupted by noise.

I. INTRODUCTION

Periodicity arises naturally in various engineering and scientific disciplines [1]. From the mechanical vibrations of a car engine to the oscillations in electronic circuits, and even the rhythmic patterns of biological processes, periodicity is a ubiquitous feature [2]–[4]. Understanding, analyzing, and controlling these periodic behaviors are essential for optimizing system performance, ensuring stability, and enhancing the predictability of various applications.

Linear time-periodic (LTP) systems, a subset of linear time-varying systems, are characterized by periodic variations in their parameters over time. Furthermore, under specific conditions, nonlinear systems can be approximated as LTP systems when linearized along a periodic trajectory [3]. Given the broad spectrum of applications, modeling LTP systems is of significant interest for both analysis and control design. LTP systems, in comparison to LTI systems, introduce a higher degree of complexity. This complexity accounts for the preference in focusing on the identification of LTI systems, a choice supported by the extensive development of tools and methodologies for this purpose [5].

Most identification techniques for LTP systems involve first identifying one or more linear time-invariant (LTI) systems, which then serve as the basis for deriving a model of the LTP system. Lifting schemes have proven successful to identify the parameters of a discrete time equivalent

LTI system either in the time domain [6] or the frequency domain [7]. The subspace identification method has also been extended to LTP systems both in the time-domain [8] and more recently in frequency-domain [9], [10]. In [10], restrictions on the input-output dimension and input form were relaxed by leveraging the idea to employ the frequency response of a time-lifted system with a linear time-invariant structure. Also, in [11], Fourier transformations of state and input data are used to identify the Fourier series coefficients of the state and input matrices. It is important to note that this approach is restricted to stable systems with oscillations that attain a steady-state, which can be a limiting factor, particularly in control applications.

Moreover, the majority of the proposed methods to date is available for discrete-time systems and, when extended to continuous-time, require unquantified approximations. Our aim is to propose a methodology to identify the Fourier coefficients of the state and input matrices of LTP systems in continuous time for both stable and unstable systems. Importantly, we aim to remove restrictions related to systems achieving a steady-state and to eliminate signal limitations. To achieve this objective, we make use of an equivalence result established in [12], linking LTP systems to infinite-dimensional LTI systems characterized by a block Toeplitz structure formed by the Fourier coefficients of the state and input matrices. LTP system’s parameters are thus inferred from the Fourier series. However, it is essential to note that the harmonic system is inherently infinite-dimensional. Consequently, truncation becomes necessary. By selecting a sufficiently high truncation order, the identification problem is translated into a finite-dimensional linear least-squares problem. We prove that the solution to this finite-dimensional problem converges to the solution of the infinite-dimensional counterpart with an arbitrarily small error.

The paper is organized as follows. The next section is dedicated to mathematical preliminaries on harmonic modelling. In Section III, we state the identification problem. The main results are established in Section IV where we tackle the approximation of the infinite-dimensional identification problem. Illustrative examples are given in Section V, demonstrating the application of our approach to identify linear time-periodic systems, even in scenarios where state measurements are affected by noise.

Notations: C^a denotes the space of absolutely continuous function, $L^p([a, b], \mathbb{C}^n)$ (resp. $\ell^p(\mathbb{C}^n)$) denotes the Lebesgues spaces of p -integrable functions on $[a, b]$ with values in \mathbb{C}^n (resp. p -summable sequences of \mathbb{C}^n) for $1 \leq p \leq \infty$. L^p_{loc} is the set of locally p -integrable functions. The

F. Vernerey, P. Riedinger and J. Daafouz are with Université de Lorraine, CNRS, CRAN, F-54000 Nancy, France. A. Iannelli is with University of Stuttgart, Institute for Systems Theory and Automatic Control.

notation $f(t) = g(t)$ *a.e.* means almost everywhere in t or for almost every t . To simplify the notations, $L^p([a, b])$ or L^p will be often used instead of $L^p([a, b], \mathbb{C}^n)$.

II. PRELIMINARIES ON HARMONIC MODELLING

For a given integer n , consider $x \in L^2_{loc}(\mathbb{R}, \mathbb{C}^n)$ a complex valued function of time. Its sliding Fourier decomposition over a window of length T is defined by the time-varying infinite sequence $X = (\dots, X_{-1}, X_0, X_1, \dots) := \mathcal{F}(x) \in C^a(\mathbb{R}, \ell^2(\mathbb{C}^n))$ (see [12]) whose n -dimensional components X_k (named k -th phasor) satisfy:

$$X_k(t) := \frac{1}{T} \int_{t-T}^t x(\tau) e^{-j\omega k \tau} d\tau$$

for $k \in \mathbb{Z}$, with $\omega := \frac{2\pi}{T}$. The Toeplitz transformation of a matrix function $A \in L^2_{loc}(\mathbb{R}, \mathbb{C}^{n \times m})$, denoted $\mathcal{A} := \mathcal{T}(A)$, defines a block Toeplitz and infinite dimensional matrix as follows:

$$\mathcal{A} := \mathcal{T}(A) = \begin{bmatrix} \ddots & & & & & & \ddots \\ & A_0 & A_{-1} & A_{-2} & & & \\ \dots & A_1 & A_0 & A_{-1} & \dots & & \\ & A_2 & A_1 & A_0 & & & \\ \ddots & & & & & & \ddots \end{bmatrix}, \quad (1)$$

where $(A_k)_{k \in \mathbb{Z}}$ denotes the phasor sequence of A .

Definition 1: We say that X belongs to H if X is an absolutely continuous function (i.e. $X \in C^a(\mathbb{R}, \ell^2(\mathbb{C}^n))$) and fulfills for any k the following condition:

$$\dot{X}_k(t) = \dot{X}_0(t) e^{-j\omega k t} \quad a.e. \quad (2)$$

Similarly to the Riesz-Fisher theorem which establishes a one-to-one correspondence between the spaces L^2 and ℓ^2 , the following theorem establishes a one-to-one correspondence between the spaces L^2_{loc} and H (see [12]).

Theorem 1: For a given $X \in L^2_{loc}(\mathbb{R}, \ell^2(\mathbb{C}^n))$, there exists a representative $x \in L^2_{loc}(\mathbb{R}, \mathbb{C}^n)$ of X , i.e. $X = \mathcal{F}(x)$, if and only if $X \in H$.

Thanks to Theorem 1, it is established in [12] that any system having solutions in Carathéodory sense can be transformed by a sliding Fourier decomposition into an infinite dimensional system for which a one-to-one correspondence between their respective trajectories is established providing that the trajectories in the infinite dimensional space belong to the subspace H . Moreover, when a T -periodic system is considered, the resulting infinite dimensional system is time-invariant. For instance, consider T -periodic functions $A(\cdot)$ and $B(\cdot)$ respectively of class $L^2([0, T], \mathbb{C}^{n \times n})$ and $L^\infty([0, T], \mathbb{C}^{n \times m})$ and let:

$$\dot{x}(t) = A(t)x(t) + B(t)u(t) \quad x(0) = x_0 \quad (3)$$

If x is a solution associated to the control $u \in L^2_{loc}(\mathbb{R}, \mathbb{C}^m)$ of the linear time periodic (LTP) system (3) then, $X := \mathcal{F}(x)$ is a solution associated to $U := \mathcal{F}(u)$ of the linear time invariant (LTI) system:

$$\dot{X}(t) = (\mathcal{A} - \mathcal{N})X(t) + \mathcal{B}U(t), \quad X(0) = \mathcal{F}(x)(0) \quad (4)$$

where $\mathcal{A} = \mathcal{T}(A)$, $\mathcal{B} = \mathcal{T}(B)$ and

$$\mathcal{N} := \text{diag}(j\omega k \otimes Id_n, k \in \mathbb{Z}) \quad (5)$$

with \otimes the Kronecker product. Reciprocally, if $X \in H$ is a solution to (4) with $U \in H$, then their representatives x and u (i.e. $X = \mathcal{F}(x)$ and $U = \mathcal{F}(u)$) are a solution to (3). In addition, it is proved in [12] that one can reconstruct time trajectories from the exact formula:

$$x(t) = \mathcal{F}^{-1}(X)(t) = \sum_{k=-\infty}^{+\infty} X_k(t) e^{j\omega k t} + \frac{T}{2} \dot{X}_0(t) \quad (6)$$

III. PROBLEM FORMULATION

We consider a continuous-time LTP system

$$\dot{x}(t) = A(t)x(t) + B(t)u(t) \quad (7)$$

where A and B are real-valued T -periodic continuous functions in $L^\infty([0, T])$, $x(t) \in \mathbb{R}^n$ and $u(t) \in \mathbb{R}^m$. Furthermore, we make the following assumptions:

Assumption 1: The period T is known and the state can be measured or estimated over a sufficiently long time interval $[t_0, t_f]$.

These assumptions are common for identification of LTP systems, see for example [11]. Building upon the preceding section, studying such LTP system essentially involves examining an equivalent infinite-dimensional Linear Time-Invariant (LTI) system as defined in (4). Indeed, as

$$A(t) = \sum_{k=-\infty}^{\infty} A_k e^{j\omega k t} \quad a.e. \quad B(t) = \sum_{k=-\infty}^{\infty} B_k e^{j\omega k t} \quad a.e.,$$

the identification of A and B can be achieved though the identification of the phasor sequences (A_k) and (B_k) that appear explicitly in the operators \mathcal{A} and \mathcal{B} in (4) (see (1)). Hence, it is possible to reformulate the task of identifying a LTP system as the task of identifying a LTI system, with the caveat that we must address the challenge of its infinite dimensionality. Consequently, the infinite-dimensional problem we aim to solve, achieving precision to an arbitrarily small error, can be stated as follows:

Problem 1: Under Assumption 1, identify \mathcal{A} and \mathcal{B} in (4) from a state/input (x, u) trajectory of system (7) and deduce A and B .

Problem 1 is an infinite dimensional one. Our goal is to provide a computationally tractable approach to identification of (4) with a guaranteed bound on the approximation. As we will see in the sequel, adopting this approach offers several noteworthy advantages. The first advantage is inherently tied to the LTI characteristic of the harmonic system, as well as the Toeplitz structure exhibited by its elements. The second advantage pertains to the filtering property achieved through the integral action for computing the phasors (X, U) from state/input trajectories (x, u) . The final advantage stems from the fact that we do not require to compute the derivative terms. Indeed, these terms satisfy the following relationship:

$$\dot{X}_k(t) = e^{-j\omega t} \dot{X}_0(t)$$

with

$$\dot{X}_0(t) = \frac{1}{T}(x(t) - x(t-T)) \quad (8)$$

(see [12]) and thus it is not necessary to compute any derivative of x . These two last properties will be very useful to generate harmonic data and simplify the identification problem.

IV. MAIN RESULTS

In this section, we show how problem 1 can be reduced to a finite dimensional least squares identification problem whose solution satisfies the original problem up to an arbitrarily small error. As a consequence, the identification of the original LTP system is achieved with a guaranteed bound on the approximation. In addition, a direct bound on the difference of the estimated and true matrices is derived.

A. A central strip identification problem

Before deriving a finite dimensional approximation to Problem 1, we start by proving some technical results.

Theorem 2: Let $A \in L^\infty([0, T])$ and the Fourier series of A given by $A(t) = \sum_{k=-\infty}^{\infty} A_k e^{j\omega kt}$ a.e. Then, the operator sequence indexed by p , $\mathcal{A}|_p(t) := \sum_{k=-p}^p A_k e^{j\omega kt}$ converges in L^∞ operator norm to A and we have:

$$\lim_{p \rightarrow +\infty} \|A - \mathcal{A}|_p\|_{L^\infty} = \lim_{p \rightarrow +\infty} \|\mathcal{A} - \mathcal{A}|_p\|_{\ell^2} = 0$$

where $\mathcal{A} := \mathcal{T}(A)$ and $\mathcal{A}|_p := \mathcal{T}(\mathcal{A}|_p)$.

Proof: First, let us recall [13] that $A \in L^\infty([0, T])$ if and only if \mathcal{A} is a bounded operator on ℓ^2 i.e. there exists C s.t.

$$\|\mathcal{A}\|_{\ell^2} = \sup_{\|x\|_{\ell^2}=1} \|\mathcal{A}x\|_{\ell^2} \leq C$$

and $\|A\|_{L^\infty} = \|\mathcal{A}\|_{\ell^2}$. Hence, using the Fourier series of A , we can write:

$$\|\mathcal{A} - \mathcal{A}|_p\|_{\ell^2} = \|A - \mathcal{A}|_p\|_{L^\infty} = \left\| \sum_{|k|>p} A_k e^{j\omega kt} \right\|_{L^\infty} \quad (9)$$

where $\mathcal{A} := \mathcal{T}(A)$ and $\mathcal{A}|_p := \mathcal{T}(\mathcal{A}|_p)$. As by assumption there exists a constant C_1 such that

$$\|\mathcal{A}\|_{\ell^2} = \|A\|_{L^\infty} = \left\| \sum_{k \in \mathbb{Z}} A_k e^{j\omega kt} \right\|_{L^\infty} < C_1$$

the series $\sum_{k \in \mathbb{Z}} A_k e^{j\omega kt}$ converges almost everywhere and $\lim_{p \rightarrow +\infty} \sum_{|k|>p} A_k e^{j\omega kt} = 0$ a.e. Taking the limit w.r.t. p in (9) leads to the result. \blacksquare

From this result, it follows that replacing the pair $(\mathcal{A}, \mathcal{B})$ by $(\mathcal{A}|_p, \mathcal{B}|_p)$ leads to the following approximation of the harmonic state dynamic:

Corollary 1: Let (x, u) be a trajectory of (7) and $(X, U) := \mathcal{F}(x, u)$. For any $\epsilon > 0$, there exists p such that for any compact time interval I

$$\sup_{t \in I} \frac{\|\Psi(X(t), U(t))\|_{\ell^2}}{\|(X(t), U(t))\|_{\ell^2}} \leq 2\epsilon \quad (10)$$

where $\Psi(X(t), U(t)) := (\mathcal{A} - \mathcal{N})X(t) + \mathcal{B}U(t) - ((\mathcal{A}|_p - \mathcal{N})X(t) + \mathcal{B}|_p U(t))$

Proof: As the operator norms are sub-multiplicative, we have for any t :

$$\begin{aligned} & \|(\mathcal{A} - \mathcal{N})X(t) + \mathcal{B}U(t) - ((\mathcal{A}|_p - \mathcal{N})X(t) + \mathcal{B}|_p U(t))\|_{\ell^2} \\ & \leq \|\mathcal{A} - \mathcal{A}|_p\|_{\ell^2} \|X(t)\|_{\ell^2} + \|\mathcal{B} - \mathcal{B}|_p\|_{\ell^2} \|U(t)\|_{\ell^2} \\ & \leq (\|\mathcal{A} - \mathcal{A}|_p\|_{\ell^2} + \|\mathcal{B} - \mathcal{B}|_p\|_{\ell^2}) \|(X(t), U(t))\|_{\ell^2} \end{aligned}$$

then, as X and U are absolutely continuous functions of the time, the supremum on any compact set exists and using Theorem 2 the result follows. \blacksquare

Definition 2: The degree $d^\circ A \in \mathbb{Z}^+ \cup \{+\infty\}$ of A is defined by the greater non vanishing phasor of A .

Corollary 1 shows that if $d^\circ A$ and $d^\circ B$ are not finite, it is always possible to obtain an accurate approximated solution to the identification problem by imposing sufficiently large $d^\circ A$ and $d^\circ B$. Indeed for a given $\epsilon > 0$ and $p(\epsilon)$ such that Corollary 1 holds, the solution (\tilde{A}, \tilde{B}) of the normalized linear least-squares optimization problem:

$$\min_{\mathcal{A}|_p, \mathcal{B}|_p} \sup_{t \in I} \frac{\|\dot{X}(t) - ((\mathcal{A}|_p - \mathcal{N})X(t) + \mathcal{B}|_p U(t))\|_{\ell^2}^2}{\|(X(t), U(t))\|_{\ell^2}^2}$$

where the unknowns $\mathcal{A}|_p, \mathcal{B}|_p$ which are block p -banded (i.e. $A_k := 0$ and $B_k := 0$ for $k > p$) and Toeplitz matrices, will necessarily satisfy relation (10).

Now, let us show that Problem 1 can be simplified and reduced to a finite dimensional problem. This problem is referred to as the "central strip identification problem," relating to the "0-row" of (4).

Theorem 3: Problem 1 can be reduced to the central strip identification problem which involves the identification of:

$$\dot{X}_0(t) = \sum_{k \in \mathbb{Z}} A_k X_{-k}(t) + \sum_{k \in \mathbb{Z}} B_k U_{-k}(t) \quad (11)$$

Moreover, if $d^\circ A$ and $d^\circ B$ are finite then the central strip identification problem reduces to the identification of:

$$\dot{X}_0(t) = \sum_{k=-d^\circ A}^{d^\circ A} A_k X_{-k}(t) + \sum_{k=-d^\circ B}^{d^\circ B} B_k U_{-k}(t)$$

which is a finite dimensional problem that involves $n^2(2d^\circ A + 1) + nm(2d^\circ B + 1)$ real unknowns.

Proof: As $\dot{X}_p(t) = e^{-j\omega pt} \dot{X}_0(t)$ for any p and as

$$\dot{X}_0(t) = \sum_{k \in \mathbb{Z}} A_k X_{-k}(t) + \sum_{k \in \mathbb{Z}} B_k U_{-k}(t),$$

it follows that the p -strip of (4) corresponding to $\dot{X}_p(t)$ satisfies

$$\dot{X}_p(t) = e^{-j\omega pt} \left(\sum_{k \in \mathbb{Z}} A_k X_{-k}(t) + \sum_{k \in \mathbb{Z}} B_k U_{-k}(t) \right)$$

and is no more informative than \dot{X}_0 . Thus, only the central strip is sufficient to identify the harmonic system (4). Moreover, if $d^\circ A$ and $d^\circ B$ are finite, there are $n^2(2d^\circ A + 1) + nm(2d^\circ B + 1)$ complex unknowns to be determined in this problem. As A and B are real-valued functions, their phasors of negative and positive order are complex conjugates of each other: $\forall k \in \mathbb{Z}, A_{-k} = \overline{A_k}$. Furthermore, as any phasor of order 0 is real-valued, this means that Problem 1 amounts

to identifying $n^2(2d^\circ A + 1) + nm(2d^\circ B + 1)$ real unknowns. ■

Finally, combining Corollary 1 and Theorem 3 leads to the following result:

Theorem 4: For any $u \in L_{loc}^2$ and any $\epsilon > 0$, there exists p such that the finite dimensional normalized central strip identification problem on interval I given by:

$$\min_{A_k, B_k, |k| \leq p} \sup_{t \in I} \frac{\|\dot{X}_0(t) - \sum_{k=-p}^p (A_k X_{-k}(t) + B_k U_{-k}(t))\|^2}{\|(X(t), U(t))\|_{\ell^2}^2} \quad (12)$$

where $\|\cdot\|$ refers to the 2-norm, leads to an approximated solution $\tilde{A}(t) := \sum_{k=-p}^p \tilde{A}_k e^{j\omega_k t}$ and $\tilde{B}(t) := \sum_{k=-p}^p \tilde{B}_k e^{j\omega_k t}$ that satisfies:

$$\sup_{t \in I} \frac{\|\dot{X}_0(t) - \sum_{k=-p}^p (\tilde{A}_k X_{-k}(t) + \tilde{B}_k U_{-k}(t))\|}{\|(X(t), U(t))\|_{\ell^2}} \leq 2\epsilon \quad (13)$$

and relation (13) still holds true if I in (12) and (13) is replaced by a discrete set $I_d \subset I$.

Proof: Let us define the central strip selecting operator $\mathcal{C}_0 := [\cdots 0 \text{ Id}_n 0 \cdots]$ such that $X_0 = \mathcal{C}X$ where $X := \mathcal{F}(x)$. Obviously $\|\mathcal{C}_0\| = 1$ where $\|\cdot\|$ is the standard Euclidian norm (2-norm) since

$$\sup_{\|X\|_{\ell^2}=1} \|\mathcal{C}_0 X\| = \sup_{\|X\|_{\ell^2}=1} \|X_0\| = 1$$

is achieved for $X = [\cdots, 0, X_0, 0, \cdots]$ with $\|X_0\| = 1$. Now, for a given u , and $\epsilon > 0$, we know that there exists p such that Corollary 1 is satisfied and thus relation (10) holds. Therefore,

$$\frac{\|\mathcal{C}_0 \Psi(X(t), U(t))\|}{\|(X(t), U(t))\|_{\ell^2}} \leq \|\mathcal{C}_0\| \sup_{t \in I} \frac{\|\Psi(X(t), U(t))\|_{\ell^2}}{\|(X(t), U(t))\|_{\ell^2}} \leq 2\epsilon. \quad (14)$$

As $\mathcal{C}_0 \Psi(X(t), U(t)) = \dot{X}_0(t) - \sum_{k=-p}^p (A_k X_{-k}(t) + B_k U_{-k}(t))$, we see that the minimizer of (12) satisfies necessarily (13). Finally, if in (12) I is replaced by a discrete set $I_d \subset I$, the minimizer of (12) satisfies necessarily (13) on I_d . ■

Remark 1: Note that computing $\|(X(t), U(t))\|_{\ell^2}$ in (12) can be simply achieved by computing $\|(x(t), u(t))\|_{L^2([t-T, t])}$ as Riesz-Fisher theorem implies

$$\|X(t)\|_{\ell^2} = \|x\|_{L^2([t-T, t])} = \left(\frac{1}{T} \int_{t-T}^t x^2(\tau) d\tau\right)^{\frac{1}{2}}.$$

Having successfully converted the infinite-dimensional harmonic identification problem into an approximate finite-dimensional counterpart, the next subsection is dedicated to the conditions essential for achieving a precise solution from a discrete-time sequence of data.

B. Solving the central strip least squares identification problem

For a sufficiently large number N , consider a sampled state/input trajectory (x, u) of the LTP system (7) with sampling time $\delta t = T/N$ over the time interval $I := [t_0, t_f]$. For a given order p , the computation of phasors $(X_k(t), U_k(t))$ for $|k| \leq p$ on the time interval $[t_0 + T, t_f]$ can be performed using

a Fast Fourier Transform. Also, \dot{X}_0 can be determined using (8). Then, these data are normalized following Remark 1 that is, for $|k| \leq p$

$$(X_k(t), U_k(t))_{\mathbf{N}} := \frac{(X_k(t), U_k(t))}{M(t)} \quad \text{and} \quad \dot{X}_{0\mathbf{N}}(t) := \frac{\dot{X}_0(t)}{M(t)}$$

where $M(t) := \|(x(t), u(t))\|_{L^2([t-T, t])}$. The data are stored as follows:

$$\begin{aligned} \mathbf{X}_1 &:= (\dot{X}_{0\mathbf{N}}(t_0 + T) \quad \cdots \quad \dot{X}_{0\mathbf{N}}(t_f)) \in \mathbb{C}^{n \times L} \\ \mathbf{X}_0 &:= (X_{-p:p\mathbf{N}}(t_0 + T) \quad \cdots \quad X_{-p:p\mathbf{N}}(t_f)) \in \mathbb{C}^{n(2p+1) \times L} \\ \mathbf{U}_0 &:= (U_{-p:p\mathbf{N}}(t_0 + T) \quad \cdots \quad U_{-p:p\mathbf{N}}(t_f)) \in \mathbb{C}^{m(2p+1) \times L} \end{aligned}$$

where $X_{-p:p\mathbf{N}}(t)$ is a column vector which contains the normalized phasors from order $-p$ to p of the n components of X , L being the number of samples. The p -banded central strip identification problem given by (12) is formulated as follows:

Problem 2: From data $(\mathbf{X}_1, \mathbf{X}_0, \mathbf{U}_0)$, solve the least-squares problem:

$$\min_{A_k, B_k, |k| \leq p} \|\mathbf{X}_1 - [A_p, \cdots, A_{-p}, B_p, \cdots, B_{-p}] \begin{bmatrix} \mathbf{X}_0 \\ \mathbf{U}_0 \end{bmatrix}\|^2 \quad (15)$$

where $\|\cdot\|$ refers to 2-norm.

We have the following proposition.

Proposition 1: The data $(\mathbf{X}_0, \mathbf{U}_0)$ are informative for system identification if and only if

$$\text{rank} \begin{pmatrix} \mathbf{X}_0 \\ \mathbf{U}_0 \end{pmatrix} = (n+m)(2p+1). \quad (16)$$

Proof: The proof follows from [14] dedicated to data informativity for noise free linear systems identification. ■

To ensure that the rank condition (16) is met, a necessary condition is that the sample size, denoted as L , exceeds the value of $(n+m)(2p+1)$.

Theorem 5: For a given p , if the data $(\mathbf{X}_0, \mathbf{U}_0)$ are informative for system identification, the solution of the least-squares problem is given by

$$[\tilde{A}_p, \cdots, \tilde{A}_{-p}, \tilde{B}_p, \cdots, \tilde{B}_{-p}] := \mathbf{X}_1 \begin{bmatrix} \mathbf{X}_0 \\ \mathbf{U}_0 \end{bmatrix}^\dagger$$

where $\begin{bmatrix} \mathbf{X}_0 \\ \mathbf{U}_0 \end{bmatrix}^\dagger$ refers to the pseudo-inverse of $\begin{bmatrix} \mathbf{X}_0 \\ \mathbf{U}_0 \end{bmatrix}$ and is uniquely determined. Moreover, for a given $\epsilon > 0$, if p satisfies Corollary 1 on $I := [t_0 + T, t_f]$ then relation (13) is satisfied at least at every sample time $t := t_k + T$ of I and we have:

$$\begin{aligned} \max_t &\|([\tilde{A}_p, \cdots, \tilde{A}_{-p}, \tilde{B}_p, \cdots, \tilde{B}_{-p}] \\ &- [A_p, \cdots, A_{-p}, B_p, \cdots, B_{-p}]) \begin{bmatrix} X_{-p:p\mathbf{N}}(t) \\ U_{-p:p\mathbf{N}}(t) \end{bmatrix}\| \leq 4\epsilon. \quad (17) \end{aligned}$$

Proof: As condition (16) is satisfied, the minimizer of (15) is uniquely defined. If p is such that Corollary 1 is satisfied on I then relation (13) is satisfied on every sample

time $t := t_k + T$ (as stated in Theorem 4). Using (13) and (14), it follows that for any sample time $t := t_k + T$:

$$\begin{aligned} & \|([\tilde{A}_p, \dots, \tilde{A}_{-p}, \tilde{B}_p, \dots, \tilde{B}_{-p}] \\ & \quad - [A_p, \dots, A_{-p}, B_p, \dots, B_{-p}]) \begin{bmatrix} X_{-p:p_N}(t) \\ U_{-p:p_N}(t) \end{bmatrix}\| \\ & \leq \left\| \sum_{k=-p}^p (\tilde{A}_k X_{-k}(t) + \tilde{B}_k U_{-k}(t)) - \dot{X}_0(t) \right\| + \\ & \quad \left\| \dot{X}_0(t) - \sum_{k=-p}^p (A_k X_{-k}(t) + B_k U_{-k}(t)) \right\| \leq 4\epsilon. \end{aligned}$$

■

Corollary 2: There is a subsequence of sampling time t_{i_k} of length $(n+m)(2p+1)$ such that the matrix V whose columns are formed by $(X_{-p:p_N}(t_{i_k}), U_{-p:p_N}(t_{i_k}))$ is invertible. Then, the following bound holds:

$$\begin{aligned} & \|([\tilde{A}_p, \dots, \tilde{A}_{-p}, \tilde{B}_p, \dots, \tilde{B}_{-p}] \\ & \quad - [A_p, \dots, A_{-p}, B_p, \dots, B_{-p}])\| \leq 4\epsilon M \end{aligned}$$

where $M = (n+m)(2p+1)\|V^{-1}\|$.

Proof: As the rank condition (16) is achieved, an invertible matrix V can be extracted from the columns of (X_0, U_0) . As for any $Y \in \mathbb{R}^r$ with $r = (n+m)(2p+1)$ s.t. $\|Y\| = 1$, there exists Λ s.t. $Y = V\Lambda$, the following relation holds (using (17)):

$$\begin{aligned} & \|([\tilde{A}_p, \dots, \tilde{A}_{-p}, \tilde{B}_p, \dots, \tilde{B}_{-p}] \\ & \quad - [A_p, \dots, A_{-p}, B_p, \dots, B_{-p}])Y\| \leq 4\epsilon \sum_i |\Lambda_i| \end{aligned}$$

Using norm equivalence in finite dimension, we have:

$$\begin{aligned} & \|([\tilde{A}_p, \dots, \tilde{A}_{-p}, \tilde{B}_p, \dots, \tilde{B}_{-p}] \\ & \quad - [A_p, \dots, A_{-p}, B_p, \dots, B_{-p}])Y\| \leq 4\epsilon r \|\Lambda\| \\ & \leq 4\epsilon r \|V^{-1}Y\| \leq 4\epsilon r \|V^{-1}\| \end{aligned}$$

Taking the supremum on Y leads to the result. ■

Remark 2: Recall that Corollary 1 primarily establishes the existence of a solution, yet it does not provide a constructive approach. Determining an appropriate value for p often entails a trial-and-error process until a satisfactory solution is achieved. Here, a satisfactory solution denotes one in which the higher-order phasors obtained approach zero. Furthermore, the rank condition (16) acts as a necessary condition for the uniqueness of a solution in Problem 2 when dealing with noise-free data. However, it is essential to highlight that this rank condition becomes insufficient in the presence of noisy measurements. To mitigate the impact of noise, a larger value for L becomes imperative in addressing Problem 2.

C. Validation

Before exploring specific examples, we introduce a validation protocol that will be applied in the following section. For theoretical validation, our initial focus is on the noiseless scenario. After successfully solving the least-squares Problem 2 for a particular value of p , the subsequent step is to validate the resulting model. Here, we employ the relative error

between the true and estimated phasors as our validation criterion. This relative error is computed as follows:

$$err := 100 \cdot \frac{\|P_{th} - P_{est}\|_2}{\|P_{th}\|_2} \quad (18)$$

where P_{th} is a matrix which contains the theoretical values of the phasors and P_{est} contains the phasors estimated with the least-squares method. A threshold ϵ must be chosen to indicate if the obtained values of the phasors are close enough to the true ones. If $err \leq \epsilon$, the estimated model is acceptable, otherwise a larger value of p must be chosen to satisfy the validation criterion.

It is crucial to recognize that in real-world scenarios, the theoretical values of the phasors are often unknown. Consequently, an alternative validation criterion must be employed. This validation procedure involves the use of a distinct dataset separate from the one used for identification. One can simulate the LTP system on a new trajectory, facilitating a comparison between the true and estimated trajectories. To assess the sensitivity of our proposed methodology to noisy data, we introduce a random disturbance to the state measurements x . At each time instant t and for every $i \in [[1, n]]$, the noise on state x_i conforms to a Gaussian distribution $N(0, \sigma^2)$ where $3\sigma = \frac{5}{100}|x_i(t)|$. We then follow the same procedure to calculate the error err .

V. ILLUSTRATIVE EXAMPLES

In this section, we illustrate our approach on three examples, one of them is the wind turbine problem borrowed from [15]. The threshold for the relative error in the phasors is set at $\epsilon = 10\%$.

A. A finite phasor-order example

First, let us consider a LTP system generated with random phasors for A and B , where $n = 3$, $m = 2$ and $d^o A = d^o B = 10$. Consequently, the truncation order can be set to $p = 10$. This leads to a total of $n(n+m)(2p+1) = 315$ unknowns. For this system, we tackle the identification problem, solving the least-squares Problem 2 with a set of 100 random initial conditions $x(t_0)$ and various piecewise-periodic input signals with phasors acquired from a normal distribution. We apply the validation protocol twice: once in the absence of noise in the data and once when a bounded disturbance is introduced as explained in the previous part.

In the absence of noise, the choice of $L = (n+m)(2p+1)$ and $\delta t = \frac{T}{4p}$ enables precise recovery of the unknown phasor values, provided that the system is sufficiently excited by the input, as indicated by the fulfillment of condition (16). In such instances, the relative error across all 100 trials remains below $10^{-6}\%$. This outcome underscores the success of the identification protocol when well-selected inputs are employed.

In the presence of noise, errors arise during the computation of $\dot{X}_0(t)$ and $X_k(t)$. Since $\dot{X}_0(t)$ is determined using formula (8), and the state noise is zero-mean, the error associated with $\dot{X}_0(t)$ also exhibits a zero-mean characteristic. The Fast Fourier transform introduces a noise-smoothing effect

during the calculation of $X_k(t)$. Consequently, if we denote the data matrices affected by noise as $\tilde{\mathbf{X}}_1$ and $\tilde{\mathbf{X}}_0$, there exist values, ε_1 and ε_0 , such that $|\mathbf{X}_1 - \tilde{\mathbf{X}}_1| \leq \varepsilon_1$ and $|\mathbf{X}_0 - \tilde{\mathbf{X}}_0| \leq \varepsilon_0$.

A larger value of L , namely $3(n+m)(2p+1)$, is chosen to ensure that a precise enough solution can be found. The relative error defined in equation (18), calculated for the identified phasors, falls within the range of 3.2% and 8.5% across all 100 trials. This level of relative error is considered acceptable, given the chosen threshold.

The validation of the identification results on a new trajectory is depicted in Fig. 1. With noise free data, the true and estimated trajectories align closely. In the presence of noise, an approximation of the true trajectories remains possible.

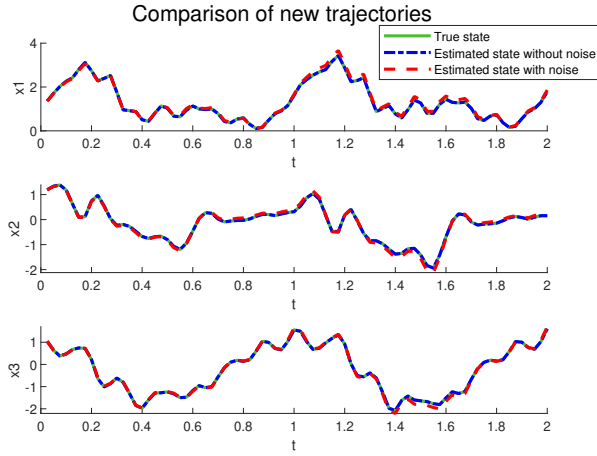


Fig. 1. Comparison of the true and estimated trajectories.

B. An infinite phasor-order example

Consider the example discussed in [16]:

$$\dot{x} = \begin{pmatrix} a_{11}(t) & a_{12}(t) \\ a_{21}(t) & a_{22}(t) \end{pmatrix} x + \begin{pmatrix} b_{11}(t) \\ 0 \end{pmatrix} u \quad (19)$$

$$a_{11}(t) = 1 + \frac{4}{\pi} \sum_{k=0}^{\infty} \frac{1}{2k+1} \sin(\omega(2k+1)t),$$

$$a_{12}(t) = 2 + \frac{16}{\pi^2} \sum_{k=0}^{\infty} \frac{1}{(2k+1)^2} \cos(\omega(2k+1)t),$$

$$a_{21}(t) = -1 + \frac{2}{\pi} \sum_{k=1}^{\infty} \frac{(-1)^k}{k} \sin(\omega kt + \frac{\pi}{4}),$$

$$a_{22}(t) = 1 - 2 \sin(\omega t) - 2 \sin(3\omega t) + 2 \cos(3\omega t) + 2 \cos(5\omega t),$$

$$b_{11}(t) = 1 + 2 \cos(2\omega t) + 4 \sin(3\omega t) \text{ with } \omega = 2\pi.$$

The corresponding Toeplitz matrix \mathcal{A} possesses an infinite number of phasors and does not exhibit a banded structure. Nevertheless, its higher-order phasors tend to converge towards zero. This convergence implies that it remains feasible to identify the non-negligible phasors within the matrix.

Given the inherent instability of this system, we employ noisy data obtained from multiple trajectories for phasor identification (see [17]). With a truncation order set at $p = 25$,

a time step of $\delta t = \frac{T}{256}$ and utilising 16 trajectories, each with a length of 512 time points, the identification error ranges from 4.6% to 9.8% among the 100 trials.

The validation of the identification results on a new trajectory is visually demonstrated in Fig. 2. It is noteworthy that the algorithm can operate with a reduced number of trajectories if their length is long enough.

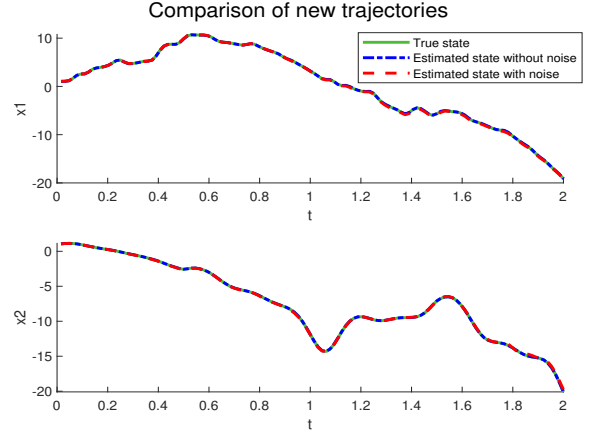


Fig. 2. Comparison of the true and estimated trajectories.

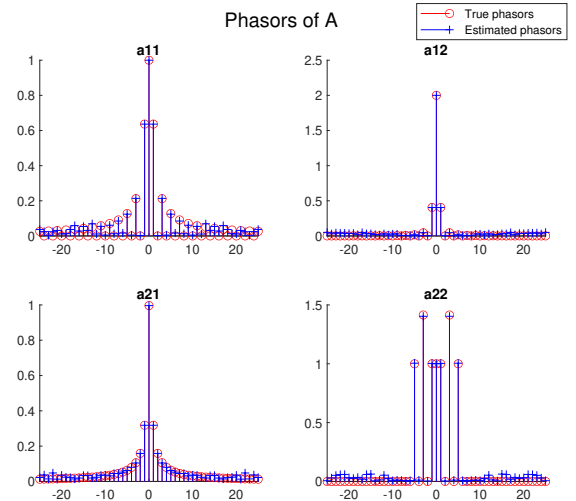


Fig. 3. Moduli of the true and estimated phasors of A with noise.

Let us plot the true and estimated moduli of the phasors for A on Fig. 3. Since we tackled the identification problem with a finite truncation order $p = 25$ and there was noise in the identification data, the effects of this noise are discernible, particularly on the higher-order phasors. This phenomenon is to be expected, as the noise injects high-frequency content into the signal. However, the amplitude of these components is obviously limited. Figure 2 shows that the predictive accuracy of the estimated phasors is already acceptable. To improve the results, a threshold can be set on the phasor modulus so that phasors below this threshold are eliminated.

In summary, even with a theoretically infinite number of phasors, it is possible to obtain an approximation for the non-negligible phasors.

C. Wind turbine

Consider the three-bladed wind turbine discussed in [15], and review its key attributes. The equation governing the system's motion can be expressed as follows:

$$M(t)\ddot{q}(t) + C(t)\dot{q}(t) + K(t)q(t) = 0$$

where M , C and K are the system's mass, damping and stiffness matrices, and $q(t) = (\zeta_1(t), \zeta_2(t), \zeta_3(t), y_c(t))^T$ contains the lag angles of each blade and the horizontal displacement of the hub. The rated rotor speed is $\Omega_r = 1.2 \text{ rad.s}^{-1}$. Functions M , C and K are periodic with period $\frac{2\pi}{\Omega_r}$. This autonomous system can be described by the state equation: $\dot{x}(t) = A(t)x(t)$ where

$$x(t) = \begin{pmatrix} q(t) \\ \dot{q}(t) \end{pmatrix}, \quad A(t) = \begin{pmatrix} 0_{4,4} & I_4 \\ -M(t)^{-1}K(t) & -M(t)^{-1}C(t) \end{pmatrix}$$

We are dealing with an unstable system characterized by $n = 8$. For this system, we embark on the identification task by solving the least-squares problem (2) across 100 random initial conditions $x(t_0)$. In this context, we assume a truncation order of $p = 4$, resulting in the determination of $n^2(2p+1) = 576$ unknowns. The step size is set to $\delta t = \frac{T}{256}$.

Given the system's inherent instability, we rely on noisy data from 15 trajectories, each with a length of 256 to identify its phasors. The identification protocol proves successful across all initial conditions, with the relative error (18) ranging from a minimum of 0.9% to a maximum of 6.3% among the 100 trials. Furthermore, the validation of these identification results on a new trajectory is depicted in Fig. 4.

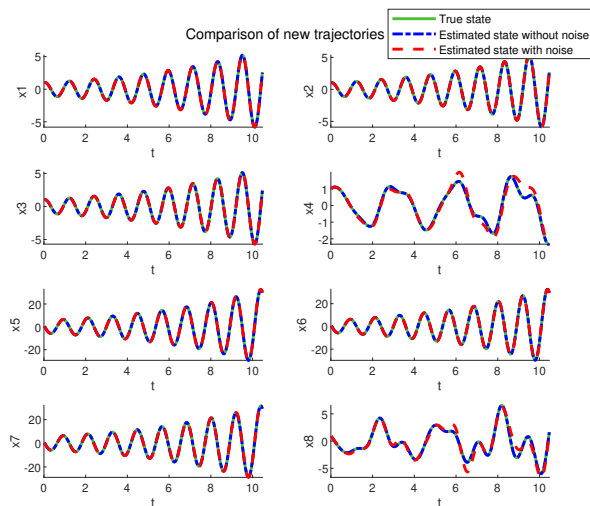


Fig. 4. Comparison of the true and estimated trajectories.

Given that the system under investigation is a wind turbine, achieving precise identification holds significant relevance, particularly in the context of control applications.

VI. CONCLUSION

In this paper, we have presented a novel approach that enables the identification of the state and input matrices of a LTP system up to an arbitrarily small error. Our approach capitalizes on the intrinsic equivalence between LTP systems in the time domain and infinite-dimensional LTI systems in the harmonic domain. Leveraging the block Toeplitz structure of the latter, we have devised a finite-dimensional linear least-squares problem, the solution of which corresponds to the unknown phasors. Our approach offers significant advantages, including avoiding signal derivative calculations, and performs effectively in noisy scenarios, as shown in numerical simulations.

REFERENCES

- [1] M. Farkas, *Periodic Motions*, vol. 104 of *Applied Mathematical Sciences*. New York, NY: Springer New York, 1994.
- [2] M. S. Allen, "Frequency-Domain Identification of Linear Time-Periodic Systems Using LTI Techniques," *Journal of Computational and Nonlinear Dynamics*, vol. 4, p. 041004, Oct. 2009.
- [3] V. Salis, A. Costabeber, S. M. Cox, and P. Zanchetta, "Stability Assessment of Power-Converter-Based AC systems by LTP Theory: Eigenvalue Analysis and Harmonic Impedance Estimation," *IEEE Journal of Emerging and Selected Topics in Power Electronics*, vol. 5, pp. 1513–1525, Dec. 2017.
- [4] S. Bittanti and P. Colaneri, *Periodic systems: filtering and control*. Communications and control engineering, London: Springer, 2009.
- [5] L. Ljung, "System identification," in *Signal analysis and prediction*, pp. 163–173, Springer, 1998.
- [6] I. Markovsky, J. Goos, K. Usevich, and R. Pintelon, "Realization and identification of autonomous linear periodically time-varying systems," *Automatica*, vol. 50, pp. 1632–1640, June 2014.
- [7] U. Saetti, J. F. Horn, T. Berger, M. J. S. Lopez, and M. B. Tischler, "Identification of Linear Time-Periodic Systems from Rotorcraft Flight-Test Data," *Journal of Guidance, Control, and Dynamics*, vol. 42, pp. 2288–2296, Oct. 2019.
- [8] M. Verhaegen and X. Yu, "A class of subspace model identification algorithms to identify periodically and arbitrarily time-varying systems," *Automatica*, vol. 31, no. 2, p. 201–216, 1995.
- [9] İ. Uyanık, U. Saranlı, M. M. Ankaralı, N. J. Cowan, and Ö. Morgül, "Frequency-domain subspace identification of linear time-periodic (LTP) systems," *IEEE Transactions on Automatic Control*, vol. 64, no. 6, pp. 2529–2536, 2018.
- [10] M. Yin, A. Iannelli, and R. S. Smith, "Subspace Identification of Linear Time-Periodic Systems With Periodic Inputs," *IEEE Control Systems Letters*, vol. 5, pp. 145–150, Jan. 2021.
- [11] İ. Uyanık, U. Saranlı, Ö. Morgül, and M. M. Ankaralı, "Parametric identification of hybrid linear-time-periodic systems," *IFAC-PapersOnLine*, vol. 49, no. 9, pp. 7–12, 2016.
- [12] N. Blin, P. Riedinger, J. Daafouz, L. Grimaud, and P. Feyel, "Necessary and Sufficient Conditions for Harmonic Control in Continuous Time," *IEEE Transactions on Automatic Control*, vol. 67, pp. 4013–4028, Aug. 2022.
- [13] I. Gohberg, S. Goldberg, and M. Kaashoek, *Classes of Linear Operators*. Operator Theory: Advances and Applications, Birkhäuser Basel, 2013.
- [14] H. J. van Waarde, J. Eising, H. L. Trentelman, and M. K. Camlibel, "Data Informativity: A New Perspective on Data-Driven Analysis and Control," *IEEE Transactions on Automatic Control*, vol. 65, pp. 4753–4768, Nov. 2020.
- [15] C. Bottasso and S. Cacciola, "Model-independent periodic stability analysis of wind turbines: Model-independent periodic stability analysis of wind turbines," *Wind Energy*, vol. 18, pp. 865–887, May 2015.
- [16] P. Riedinger and J. Daafouz, "Solving infinite-dimensional Harmonic Lyapunov and Riccati equations," *IEEE Transactions on Automatic Control*, 2022.
- [17] H. J. van Waarde, C. De Persis, M. K. Camlibel, and P. Tesi, "Willems' fundamental lemma for state-space systems and its extension to multiple datasets," *IEEE Control Systems Letters*, vol. 4, no. 3, pp. 602–607, 2020.